A R C H I V E S O F M E T A L L U R G Y A N D M A T E R I A L S
Volume 58 2013 Issue 1
DOI: 10.2478/v10172-012-0173-6

L. BLACHA*, R. BURDZIK**, A. SMALCERZ***, T. MATUŁA*

EFFECTS OF PRESSURE ON THE KINETICS OF MANGANESE EVAPORATION FROM THE OT4 ALLOY

WPŁYW CIŚNIENIA NA KINETYKĘ PROCESU ODPAROWANIA MANGANU ZE STOPU OT4

In the paper, results of the study on manganese evaporation from the OT4 alloy are presented. In the experiments, the effects of pressure on the manganese evaporation kinetics and the stages that limit the evaporation rate were investigated. It was demonstrated that the rate of manganese evaporation from the alloy increased with pressure reduction in the system. When the pressure decreases from 1000 Pa to 10 Pa, the value of overall mass transfer k_{Mn} increases from $3.9 \cdot 10^{-6}$ ms^{-1} to $208.4 \cdot 10^{-6}$ ms^{-1}. At the same time, the manganese fraction in the alloy decreased from 1.49% mass to 0.045% mass. Within the whole pressure range, the analysed evaporation process is diffusion-controlled. For pressures above 50 Pa, the determining stage is transfer in the gaseous phase, while for pressures below 50 Pa, it is transfer in the liquid phase.

Keywords: vacuum induction melting, Ti-Al-Mn alloy, evaporation, mass transfer coefficient

W prezentowanym opracowaniu przedstawiono wyniki badań odparowania manganu ze stopu OT4. W ramach prowadzonych eksperymentów badano wpływ ciśnienia na kinetykę procesu odparowania manganu i jednocześnie określono etapy limitujące jego szybkość. Wykazano, że szybkość procesu odparowania manganu ze stopu rośnie wraz z obniżaniem ciśnienia w układzie. Przy obniżeniu ciśnienia od 1000 Pa do 10 Pa wartość ogólnego współczynnika transportu masy k_{Mn} rośnie od $3.9 \cdot 10^{-6}$ ms^{-1} do $208.4 \cdot 10^{-6}$ ms^{-1}. Jednocześnie następowało obniżenie zawartości manganu w stopie od 1.49% mas. do 0.045% mas.. W całym zakresie ciśnień analizowany proces parowania ma kontrolę dyfuzyjną. Dla ciśnień powyżej 50 Pa etapem determinującym jest transport w fazie gazowej, a dla ciśnień poniżej 50 Pa transport masy w fazie ciekłej.

1. Introduction

At present, each industrial branch focuses on innovations. The subjects of innovative activities may be products, technological processes, company organisation and management systems. Innovative activities are mostly forced by the market and regarding their beneficial results, they add to a better quality of products, enhanced production as well as often cost reduction and a less negative impact of a specific technological process on the environment [1-3].

Also, innovations hold a clear position in the area of new material manufacturing. Improvements in this field are currently far more frequently observed than in the past. This is due to new design technologies, new research methods and advanced production technologies [4]. Examples of such material development are light titanium-based alloys – in recent years, a marked increase in their application has been observed. At present, the materials are utilized in the civil aviation and military aircraft, energy, chemical and automotive industries as well as medicine.

For melting processes of titanium and its alloys, the state-of-art arc, plasma, electron-beam and induction furnaces are used. The major problems with smelting of these materials are related to their strong reactivity in the liquid phase with virtually all melting pot materials, including particularly resistant thorium and calcium oxides. For this reason [5, 6], the smelting process should be performed in chilled copper melting pots and a cold melting pot (so-called "skull crucible"), obtained from molten material with highly intensive heat evacuation, is particularly convenient. Another problem regarding titanium alloy smelting is an unfavourable process of alloy component evaporation due to a high melting temperature of the alloys and significant differences in vapour pressures of their individual components. It is clearly seen during Ti-Al-X alloy smelting and casting processes when the aluminium and other volatile element contents are reduced. In the literature, study results mostly concerning aluminium losses during titanium-aluminium-vanadium and titanium-aluminium-niobium alloy smelting are available [7–10]. In the present paper, results of a study on manganese

* SILESIAN UNIVERSITY OF TECHNOLOGY, FACULTY OF MATERIALS ENGENEERING AND METALLURGY, DEPARTMENT OF METALLURGY, 40-019 KATOWICE, 8 KRASIŃSKIEGO STR., POLAND
** SILESIAN UNIVERSITY OF TECHNOLOGY, FACULTY OF TRANSPORT, DEPARTMENT OF AUTOMOTIVE VEHICLE CONSTRUCTION, 40-019 KATOWICE, 8 KRASIŃSKIEGO STR., POLAND
*** SILESIAN UNIVERSITY OF TECHNOLOGY, FACULTY OF MATERIALS ENGENEERING AND METALLURGY, DEPARTMENT OF MANAGEMENT AND COMPUTER SCIENCE, 40-019 KATOWICE, 8 KRASIŃSKIEGO STR., POLAND

evaporation from the OT4 alloy are presented. The alloy is utilized in i.a. aerospace and energy industries as well as for production of chemical equipment. The material is also increasingly often used for implant production [11, 12].

In the experiments, the effects of pressure on the evaporation kinetics of this alloy and the stages that limit the evaporation rate were investigated.

2. Authors' own study

For the experiments, the OT4 alloy was used (see Table 1 for the alloy composition).

TABLE 1
Chemical composition of the OT4 alloy used in the study

Alloy labelling	Basic alloy component fractions, %mass					
	Ti	Al	Mn	Fe	Si	Zr
Ti-4Al-2Mn	94.20	3.50	1.49	0.30	0.12	0.30

All experiments were performed in a vacuum induction furnace. The device, manufactured by Seco Warwick S.A., is designed for metal smelting at high vacuum. Additionally, it is equipped with an in-smelting sampling system.

TABLE 2
Final alloy compositions after smelting in the vacuum induction furnace

No.	Temperature, K	Pressure, Pa	Final metal fractions in the alloy, % mass		
			Ti	Al	Mn
1	1973	1000	95.433	2.633	1.330
2	1973	1000	95.400	2.680	1.370
3	2023	1000	95.367	2.643	1.34
4	2023	1000	95.400	2.650	1.360
5	1973	100	96.000	2.667	0.693
6	1973	100	96.000	2.690	0.690
7	2023	100	95.967	2.743	0.584
8	2023	100	96.200	2.600	0.597
9	1973	50	96.067	2.767	0.494
10	1973	50	96.100	2.710	0.464
11	2023	50	96.367	2.770	0.349
12	2023	50	96.401	2.740	0.349
13	1973	10	96.333	2.910	0.079
14	1973	10	96.300	2.920	0.082
15	2023	10	96.467	2.803	0.048
16	2023	10	96.500	2.770	0.045

Each experiment began with introducing an alloy sample (about 1000 g) to the graphite melting pot placed in the induction coil of the furnace. After closing the furnace, pre-specified vacuum was generated with the use of a pump system, i.e. the mechanical, diffusion and Roots pumps. When the pressure level was stabilized, the melting pot was heated up to the required temperature and the metal bath was held for 600 sec. During each smelting experiment, metal samples were collected and analysed for titanium, aluminium and manganese fractions. The experiments were performed at 5 Pa to 1000 Pa for 1973 K and 2023 K. In Table 2, sample final alloy compositions are presented.

3. Kinetic analysis

Kinetically, the process of manganese evaporation from the analysed OT4 alloy consists of three essential stages:

- transfer of manganese in the liquid phase to the interface (liquid metal surface),
- evaporation reaction on liquid Mn_l – Mn_g surface,
- transfer of gaseous manganese mass from the evaporation surface to the core of gaseous phase.

The overall mass transfer coefficient (k) in the analysed evaporation process is determined by the following equation:

$$\frac{1}{k} = \frac{1}{\beta^l} + \frac{1}{\phi k_e} + \frac{RT}{\phi \beta^g} \tag{1}$$

where:

$$\phi = \frac{p_i^o \cdot \gamma_i \cdot M_m}{\rho_m} \tag{2}$$

and: β^l – the mass transfer coefficient in the liquid phase,

β^g – the mass transfer coefficient in the gaseous phase,

k_e – the evaporation rate constant,

R – the gas constant,

T – the temperature,

M_m; ρ_m – the molar mass and density of the basic alloy component, respectively.

The value of overall mass transfer coefficient k can also be determined based on the experimental results, as follows:

$$2,303 \log \frac{C_{Mn}^t}{C_{Mn}^o} = -k \cdot \frac{F}{V}(t - t_o) \tag{3}$$

where: F – the evaporation areas (interface),

V – the liquid metal volume,

$(t - t_o)$ – the process duration,

C_{Mn}^t – the manganese concentration in the alloy after time t,

C_{Mn}^0 – the initial manganese concentration in the alloy.

In Table 2, the values of manganese overall transfer coefficient, determined with the use of equation (3) for the analysed evaporation process, are presented.

For proper identification of the stage that determines the evaporation rate, the values of β^1, β^g and k_e coefficients must be known.

In order to estimate the β^l coefficient during induction stirring of the metal bath, the following equation is mostly used:

$$\beta^l = \left(\frac{8 D_{AB} \cdot \nu_m}{\pi \cdot r_m} \right)^{0,5} \tag{4}$$

where: D_{AB} – the interdiffusion coefficient in the liquid phase,

ν_m – the near surface velocity of induction-stirred liquid metal,

r_m – the radius of liquid metal surface (assumed to be the melting pot inner radius).

The value of near surface velocity v_m is necessary for determination of the β^l coefficient value. As demonstrated in many studies, it depends on the temperature, alloy composition as well as the melting pot's position in the furnace coil and the working frequency of the device [13, 14].

The value of near surface velocity v_m was determined as follows:

$$v_m = v_1 + (v_2 - v_1)(T - T_1)/(T_2 - T_1) \quad (5)$$

where, respectively, $v_1 = 0.06$ m·s^{-1} and $v_2 = 0.21$ m·s^{-1} and $(T_2 - T_1) = 300$ K [15].

Due to the lack of literature data concerning manganese diffusion in liquid titanium, its value was estimated with the use of Darken's equation. The values of titanium and manganese self-diffusion were, respectively: $D_{Ti} = 5.3 \cdot 10^{-9}$ m^2·s^{-1} and $D_{Mn} = 7.8 \cdot 10^{-9}$ m^2·s^{-1} [16, 17].

In Table 3, the values of manganese transfer coefficient in the liquid phase, determined with the use of equation (4), are presented.

TABLE 3
Values of overall mass transfer coefficient k as well as β^1 and k'_e coefficients

No.	Temperature, K	Pressure, Pa	$\beta^1 \cdot 10^6$ m s^{-1}	$k_e \cdot 10^6$ m s^{-1}	$k_{Mn} \cdot 10^6$ m s^{-1}
1	1973	1000	198	2340	5.3
2	1973	1000	198	2340	3.9
3	2023	1000	223	3300	5.4
4	2023	1000	223	3300	4.0
5	1973	100	198	2340	45.0
6	1973	100	198	2340	52.8
7	2023	100	223	3300	61.2
8	2023	100	223	3300	53.0
9	1973	50	198	2340	66.1
10	1973	50	198	2340	70.4
11	2023	50	223	3300	89.3
12	2023	50	223	3300	88.3
13	1973	10	198	2340	153.3
14	1973	10	198	2340	176.0
15	2023	10	223	3300	205.1
16	2023	10	223	3300	208.4

The evaporation rate constant k'_e can be determined based on the following equation [18, 19]:

$$k'_e = k_e \cdot \phi = \frac{\alpha}{(2\pi RTM_i)^{0.5}} \cdot \phi \quad (6)$$

In Table 3, the values of evaporation rate constant k'_e, determined with the use of the equation (6), are also presented.

In order to estimate the φ coefficient in the equation (2), the manganese activity coefficient value was assumed as $\gamma_{Mn} = 1.53$. It was determined based on the data obtained by Kostova and Zivkovic [12].

The liquid titanium density was determined as follows [20]:

$$\rho_{Ti} = 4.208 - 5.08 \cdot 10^{-4}(T - 1941) \quad (7)$$

The equilibrium pressures over pure Ti, Al and Mn components were determined based on known standard free enthalpies of the evaporation reactions, $\Delta_p G_i^o(T)$. The values were obtained from the HSC Chemistry 6 thermodynamic database. The equilibrium pressure values were: 0.53 Pa for T=1973 K and 1.04 Pa for T=2023 K.

4. Discussion of results

While analysing the effects of pressure on the rate of manganese evaporation from the OT4 alloy, it was observed that with reduction of pressure in the measuring system from 1000 Pa to 10 Pa, the overall mass transfer k_{Mn} values increased from $3.9 \cdot 10^{-6}$ ms^{-1} to $208.4 \cdot 10^{-6}$ ms^{-1}. At the same time, the manganese fraction in the alloy decreased from 1.49% mass to 0.045% mass.

Within the pressure range above 100 Pa, a weaker impact of pressure on the analysed process rate compared to the range of 10 Pa to 100 Pa was observed (Fig. 1).

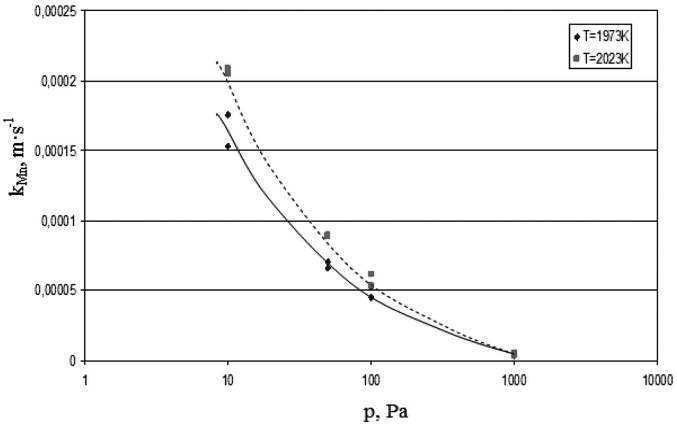

Fig. 1. Effects of pressure on the manganese overall mass transfer coefficient k_{Mn}

The resistance values regarding individual process stages were determined with the use of the equation (1), based on the estimated β^1 and k_e, values. It was seen that with pressure reduction in the system, the fraction of resistance related to mass transfer in the liquid phase in the overall manganese evaporation resistance significantly increased. It is illustrated by the data presented in Fig. 2. For 1000 Pa, the fraction is 5% and for 10 Pa, it is about 85%.

The fraction of resistance related to evaporation in the overall process resistance within the analysed pressure range did not exceed 8% (Fig. 3), mainly due to high values of manganese vapour pressure over the analysed liquid OT4 alloy.

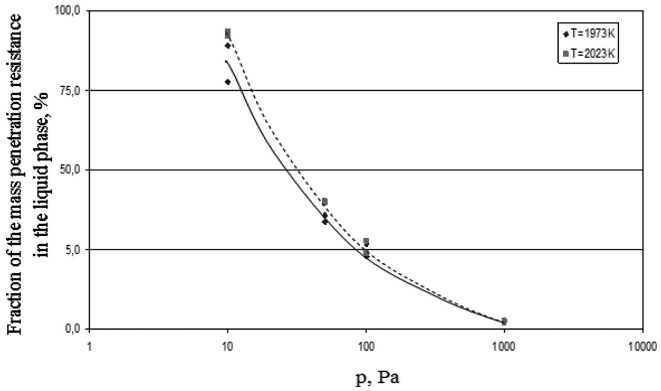

Fig. 2. Fraction of mass transfer resistance in the liquid phase with regard to the manganese overall evaporation resistance

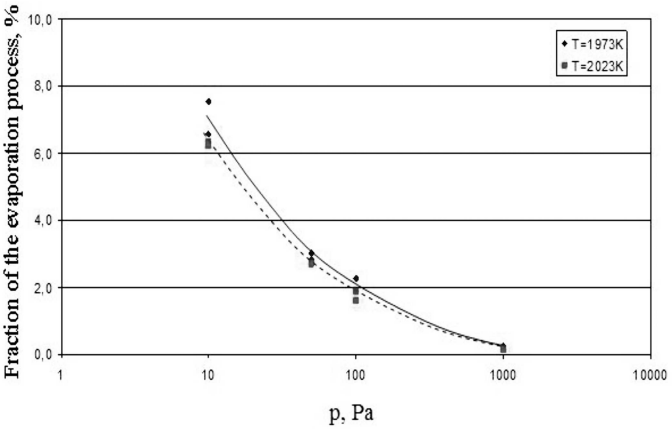

Fig. 3. Fraction of the evaporation reaction resistance on the liquid alloy surface in the manganese overall evaporation resistance

The analysis of obtained data also showed that with reduced pressure in the system, the fraction of resistance related to mass transfer in the gaseous phase in the overall manganese evaporation resistance decreased. It is illustrated by the data presented in Fig. 4. For 1000 Pa, the fraction was above 95% and for 10 Pa, it was about 5%.

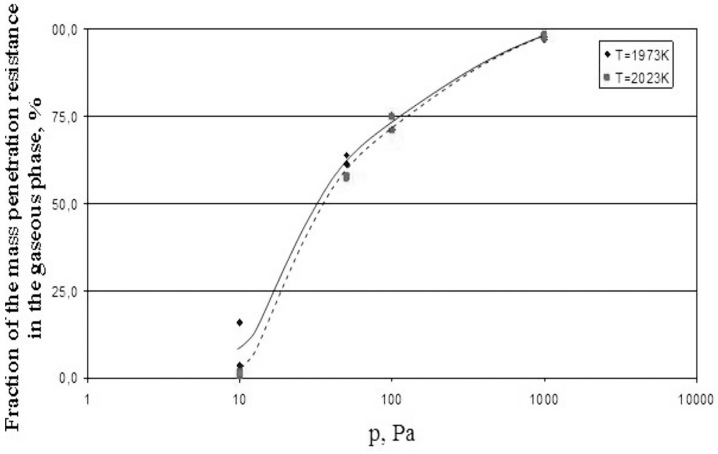

Fig. 4. Fraction of mass transfer resistance in the gaseous phase with regard to the manganese overall evaporation resistance

5. Conclusions

Based on the results of OT4 alloy remelting at 1973 K and 2023 K as well as at 10-1000 Pa in the vacuum induction furnace, the following was demonstrated:

- The smelting process at reduced pressure is accompanied by an unfavourable phenomenon of manganese evaporation due to high manganese vapour pressures over liquid alloy compared to the titanium and aluminium pressures.
- The rate of manganese evaporation from the alloy increases with pressure reduction in the system. When the pressure decreases from 1000 Pa to 10 Pa, the value of overall mass transfer coefficient k_{Mn} increases from $3.9 \cdot 10^{-6}$ ms^{-1} to $208.4 \cdot 10^{-6}$ ms^{-1}. At the same time, the manganese fraction in the alloy decreased from 1.49% mass to 0.045% mass.
- Within the pressure range above 100 Pa, a weaker impact of pressure on the analysed process rate compared to the range of 10 Pa to 100 Pa was observed.
- Within the whole pressure range, the analysed evaporation process is diffusion-controlled. For pressures above 50 Pa, the determining stage is transfer in the gaseous phase, while for pressures below 50 Pa, it is transfer in the liquid phase.
- The fraction of resistance related to evaporation in the overall process resistance within the analysed pressure range is small and did not exceed 8%.

Acknowledgements

The study was conducted under the Research Project No. N N508 589439, financed by the Ministry of Science and Higher Education – Poland.

REFERENCES

[1] K. Pałucha, Wybrane problemy zarządzania innowacjami w obszarze przygotowania i uruchamiania produkcji, in the collective work edited by J. Pyki, Koncepcje, metody i narzędzia współczesnego zarządzania, TNOiK, Katowice, 362-375 (2011).

[2] K. Pałucha, Selected problems of development of the steel industry in Poland, Metalurgija **51** (3), 357-360 (2012).

[3] A. Karbownik, Ł. Dohn, K. Sienkiewicz-Malyjurek, Value chain analysis of environmental management in urban – case study, Metaropolitan association of Upper Silesia, Polish Journal of Environmental Studies **21**, 911-921 (2012).

[4] P. Folęga, G. Siwiec, Numerical analysis of selected materials for flexsplines, Archives of Metallurgy and Materials **57** (1), 185-191 (2012).

[5] A. Szkliniarz, W. Szkliniarz, Assessment quality of Ti alloys melted in induction furnace with ceramic crucible, Solid State Phenomena **176**, 139-148 (2011).

[6] W. Szkliniarz, A. Szkliniarz, The chemical composition and microstructure of Ti-47Al-2W-0.5Si alloy melted in ceramic crucibles, Solid State Phenomena **191**, 211-220 (2012).

[7] G. Jinjie, J. Jun, S.L. Yuan, L. Guizhong, S. Yanqing, D. Hongsheng, Evaporation behavior of aluminium during the cold crucible induction skull melting of titanium

-aluminium alloys, Metallurgical and Materials Transactions B **31B**, 837-844 (2000).

[8] T. Isawa, H. Nakamura, K. Murakami, Aluminum evaporation from titanium alloys in EB hearth melting, ISIJ International **32** (5), 607-615 (1992).

[9] A. Fleszar, J. Mizera, R.Y. Fillit, T. Wierzchoń, The influence of the residual stresses on the corrosion and wear resistance of nitrated layers produced isothermally and cyclically on Ti-1Al- 1Mn titanium alloy under glow discharge conditions, Vacuum **57**, 405-410 (2000).

[10] G. Siwiec, Elimination of aluminium during the process of Ti-6Al-4V alloy, smelting in a vacuum induction furnace, Archives of Metallurgy and Materials **57** (4), 951-956 (2012).

[11] D. Krupa, J. Baszkiewicz, E. Jezierska, J. Mizera, T. Wierzchoń, A. Barcz, R. Fillit, Effect of nitrogen-ion implantation on the corrosion resistance of OT-4-0 titanium alloy in 0.9% NaCl environment, Surface & Coatings Technology **111** (1), 86-91 (1999).

[12] A.I. Kostov, D.T. Zivkovic, Thermodynamic calculations in ternary titanium-aluminium-manganese system, Journal of the Serbian Chemical Society **73** (4), 499-506 (2008).

[13] L. Blacha, J. Łabaj, Factors determining the rate of the process of metal bath components evaporation, Metalurgija **51** (4), 529-533 (2012).

[14] R. Przyłucki, S. Golak, B. Oleksiak, L. Blacha, Influence of an induction furnace's electric parameters on mass transfer velocity in the liquid phase, Metalurgija **51** (1), 67-70 (2012).

[15] J. Guo, G. Liu, Y. Su, H. Ding, J. Jia, H. Fu, Evaporation of multi-components in Ti-25Al-25Nb melt during induction skull melting process, Trans. Nonferrous Met. Soc. China **12** (4), 587-591 (2002).

[16] A. Aguero, J.M. Albella, M.P. Hierro, J. Philibert, F.J. Perez Trujillo, Self diffusion in liquid titanium, Defect and Diffusion Forum **289**, 609-614 (2008).

[17] E.S. Lewin, W.N. Zamaraew, L.W. Geld, Koefficienty wjazkosti, samodiffuzii i udelnogo elektrosoprotiwlenija żidkogo marganca, Metałły **2**, 113-116 (1976).

[18] L. Blacha, Bleientfernung aus kupferlegierungen im prozess der vakuumraffination, Archives of Metallurgy **48** (1), 105-127 (2003).

[19] J. Łabaj, Kinetics of copper evaporation from the Fe-Cu alloys under reduced pressure, Archives of Metallurgy and Materials **57** (1), 165-172 (2012).

[20] H.P. Wang, S.J. Yang, B.B. Wei, Density and structure of undercooled liquid titanium, Chinese Science Bulletin **57**, 719-723 (2012).

Received: 10 February 2012.